TRANSNAV
http://www.transnav.eu
the International Journal
on Marine Navigation
and Safety of Sea Transportation
Volume 14
Number 3
September 2020
DOI: 10.12716/1001.14.03.11

Mobile Radio Beacons in Coastal Reserved Navigation System for Ships

J.M. Kelner & C. Ziółkowski
Military University of Technology, Warsaw, Poland

ABSTRACT: At the turn of the 20th and 21st centuries, Global Navigation Satellite Systems (GNSSs) dominated navigation in air, sea, and land. Then, medium-range and long-range terrestrial navigation systems (TNSs) ceased to be developed. However, with the development of GNSS jamming and spoofing techniques, the TNSs are being re-developed, such as the Enhanced Loran. The Polish Ministry of Defense plans to develop and implement a medium-range backup navigation system for the Polish Navy which will operate in the Baltic coastal zone. This plan is a part of the global trend. This paper presents the concept of a reserve TNS (RNS) that is based on the signal Doppler frequency (SDF) location method. In 2016, the concept of the RNS, which is based on stationary radio beacons located on coastal lighthouses, has been presented. From the military viewpoint, the use of the mobile radio beacons, which may change their location, is more justified. Therefore, the paper presents an idea of using the mobile beacons for this purpose. In this paper, effectiveness of the mobile RNS is shown based on simulation studies.

1 INTRODUCTION

At the beginning of the 20th century, the use of radio waves caused the genesis of the wireless communications era. Soon after, the same radio waves contributed to revolutionizing navigation. In this way, the era of radio-navigation began. Its origins are mainly hyperbolic terrestrial navigation systems (TNSs). For this type of systems, we can include the Decca Navigator System, Consol, Omega, Syledis, Loran-A, Loran-C, Chayka, and Jemioluszka [1–6]. The TNSs were mainly used in sea and air transport. In addition, ground-based augmentation systems (GBASs) were developed mainly for aviation, e.g., the ILS, MLS, DME, VOR, and TACAN [7].

In the late 1970s, the United States developed the first navigation satellite system (NSS), i.e., the Transit, also known as the Navy NSS or NAVSAT [5]. The positioning in the Transit was based on the Doppler effect. His successor is the GPS–NAVSTAR (Global Positioning System – Navigation Signal Timing and Ranging), i.e., the first global NSS (GNSS), which is widely used in civil applications [1,8,9]. At present, the GNSSs have dominated determining the position and direction of objects' movement in both air, sea, and land transport. The Russian GLONASS and European Galileo are also counted among the GNSSs [1,8,9]. In addition, regional NSSs (RNSSs) are available in certain regions of the world, including the Chinese BeiDou (BDS), Japanese QZSS, Indian NAVIC [1,8,9]. From 2020, the BDS will gain the status of the global system. Positioning in the GNSSs and RNSSs is based on time of arrival (TOA) measurements and a multilateration method, popularly known as a time difference of arrival (TDOA) [10]. In this case, a point localization in space using the TDOA requires receiving a signal from at

least four satellites of the NSS. This method is the basis of most hyperbolic systems, including the TNSs. Additionally, the GNSSs and RNSSs use code-division multiple access (CDMA) technique, with the exception of the GLONASS, which is based on frequency-division multiple access (FDMA) [9]. Satellite-based augmentation systems (SBASs) [1,8,9] are widely used in aviation and also in maritime [11]. To the SBASs, we may include, i.a., the American WAAS, European EGNOS, Japanese MSAS, Indian GAGAN, Russian SDCM, and Chinese SNAS. For supporting systems, the French DORIS (Doppler Orbitography and Radio-positioning Integrated by Satellite) is also included [12]. This system based on the Doppler effect ensures high positioning accuracy.

A space segment is an essential part of all satellite systems. In that, the availability of the system over a whole or major area of the Earth is assured. However, this issue causes the costs of implementing and maintaining such systems are very high. Most of the GNSSs and RNSSs are military systems with the possibility of commercial civil applications. The Galileo and QZSS are only civilian systems. The availability of receiving devices, coverage for the NSSs, and high positioning precision in relation to the TNSs caused that at the end of the 20th century, most of the TNSs ceased to be supported and operated. While the GBASs are still used. Currently, the eLoran is the only operating TNS [13,14]. It consists of about forty stations located mainly along the coasts of the United States, the European Union, and Southeast Asia. This provides coverage for the northern parts of the Indian, Pacific, and Atlantic Oceans.

Over the past thirty years, we have been observing the rapid development of the GNSSs. At the same time, the development of mobile cellular networks has provided access to cheap and universal GPS receivers in smartphones. These two aspects have resulted in the dissemination of the satellite navigation and location-based services (LBSs) [15], especially in civilian land traffic. On the other hand, the widespread use of the NSSs is a secondary reason for reducing the security of countries that do not have their own NSS, as well as those that provide such the system. Lowering safety results from several premises. First, the military GNSS administrator may cause the signal to be turned off or decreasing the positioning accuracy for civilians in a specific area, e.g., military operations. In this case, military users can use code signals unavailable to civilians. Secondly, elements of the ground control or space segments may be destroyed by the enemy. Thirdly, at the last time, dynamic development of jamming and spoofing techniques dedicated to the GNSS is observed [16–19]. In this case, the use of the satellite navigation may be impossible or cause false results. The second and third reasons are a serious threat to military systems, including those countries that have own GNSS or RNSS. On the other hand, the aforementioned development of GNSSs resulted in the break of the support and development of alternative positioning methods, such as the TNSs.

In recent years, the development of the new TNSs is again considered seriously by many countries, especially for army needs in a period and area of military operations. For example, in 2012, the Armament Inspectorate of the Polish Ministry of Defense resumed an analytical-conceptual phase in development terms of "The medium-range radio-navigation system for the Polish Navy" [20]. The result of these activities is the "The medium-range mobile radio-navigation system" developed currently by the Research and Development Center for Maritime Technology [21]. This system will be based on the effects of a research team from the Gdańsk University of Technology. This team has developed the TDOA-based asynchronous and self-organizing navigation system called the AEGIR [22–24]. The work undertaken by the NATO Science & Technology Organization (STO) and the European Defense Agency in the area of "Navigation in GNSS denied environment" is another premise in this direction [25–27]. However, a monitoring system of own combat units' location named the blue force tracking (BFT) [28–31] belongs to the priorities of modernization of the Polish Army. In this case, the positioning the soldiers, equipment, and units of own forces in the absence of the GNSS access is also considered.

In 2016, a proposal to use a coastal radio-beacon (RB) system and the signal Doppler frequency (SDF) location method for positioning ships in a coastal zone was presented [20]. The SDF method [32–34], like the previously mentioned Transit and DORIS, as well as the COSPAS-SARSAT [35,36], a satellite system used in search and rescue (SAR) operations, are based on the Doppler effect. In [20], the results of simulation studies for scenarios in the Baltic Sea are presented. The use of the stationary RBs is a good solution in peacetime. However, in the case of the military operations, the reserved radio-navigation system should base on mobile RBs. The purpose of this paper is to present the concept of a mobile reserve navigation system (MRNS) for ships in the coastal zone. The effectiveness of vessel positioning using the developed system is presented based on simulation studies.

The remainder of the paper is organized as follows. In Section 2, the characteristics of the transmitting and receiving parts of the MRNS and the SDF method are presented. Section 3 contains a description of a scenario and assumptions for simulation studies. The simulation results illustrating the accuracy of the ship positioning are shown in Section 4. The paper is finished with final remarks and a summary.

2 MOBILE RESERVED NAVIGATION SYSTEM

2.1 *System Concept*

In general, the concept of the MRNS is based on the assumptions of the stationary reserved TNS for ships, which are presented in [20], i.e.,

- the system consists of several or dozen RBs operating in an asynchronous broadcasting mode,
- multi-antenna and multi-frequency-channel receiving system located on the ship enables simultaneous analysis of signals from the several RBs,
- the SDF is used to determine the position of the ship, i.e., the position of a reference receiving antenna on this ship.

The significant differences between the stationary and mobile versions mainly concern the transmitting part of the system. Stationary beacons are the core of the system presented in [20]. Their deployment was planned in existing coastal infrastructure. Considering propagation properties of radio waves, we proposed using lighthouses as points located high above sea level. In the MRNS, the RBs are placed on vehicles that can change position. Each new position brings changes in the transmitting signal.

A detailed description of the mobile RB is presented in Section 2.2. The receiving part of the system located on the ship is described in Section 2.3. In Section 2.4, the SDF implementation method in the receiving part of the MRNS is contained.

2.2 *Transmitting part of system*

The transmitting part of the MRNS consists of K mobile RBs. The concept of the RB is depicted in Figure 1.

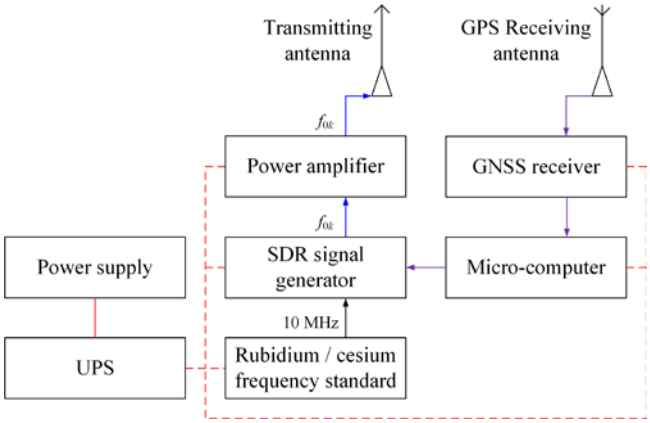

Figure 1. Structure of mobile RB

The main components of the transmitting part are identical to those in the stationary version of the RB [20], i.e., the transmitting antenna, power amplifier, and signal generator.

The generator should be made in the software-defined radio (SDR) technology [37–39] in order to be able to transmit different signal structures (waveforms). In this case, emitting the current position of the RB is important. In the stationary system, the RB transmits one type of the signal because its position is fixed. The microcomputer connected to the SDR transmitter provides the ability to generate the broadcasting signals with information about the current position of the RB.

The RB devices are placed on board a wheeled vehicle. The proposed MRNS is based on the Doppler effect. Therefore, the frequency stability of each signal source is very important [40]. Hence, we suggest equipping each RB with a rubidium or cesium frequency standard.

In order to ensure a larger operation range of the RB, each vehicle should be equipped with a hydraulic or pneumatic telescopic (locking) mast. These masts allow increasing the antenna height up to 50 m. Therefore, the vehicle should be also equipped with hydraulic stabilizers using in technical vehicles. The stabilizers are necessary to ensure stable operation of the mobile RB in different weather conditions, e.g., strong wind, stormy weather, etc. A time of assembly and disassembly of the antenna mast should be as short as possible, which will allow for a quick change of the vehicle location.

Knowing the exact position of the RB is essential for its proper operation. Hence, the identification of potential points on the coast, from which the RB may transmit the signal, is required. At such points, averaged position measurements using the GNSS should be performed in the peacetime. In the field, appropriate marking of these points should be introduced, e.g., similar to geodetic reference points (benchmarks). This point may explicitly give geographic coordinates, e.g., on a nameplate or only a benchmark number associated with the coordinates in the system. This approach allows the use of the mobile RBs in GNSS-denied conditions.

In addition, the RB should be equipped with a GNSS receiver to operate in availability conditions of the GNSS signal. We may imagine a scenario of using the MRNS when the GNSS is available on land and jamming or spoofing at a sea. In this case, the RB may emit the signals from any unmarked point on the coast. Then, the GNSS receiver should be connected to the SDR generator via the microcomputer. The GNSS receiver antenna should be placed outside the vehicle and an application that controls the waveform generation should provide an appropriate coordinate conversion between the GNSS and RB antennas.

In addition to an onboard power supply of the RB components, the vehicle should be equipped with a backup power source, e.g., an engine generator and uninterruptible power supply (UPS).

In [20], we assumed that individual RBs transmit phase-shift keying (PSK) signals. The location methodology of a PSK signal source using the SDF is presented in [41].

2.3 *Receiving part of system*

The receiving part of the MRSN is not changed compared to the stationary system presented in [20]. In Figure 2, an exemplary arrangement of the receiving antennas (RAs) on the shipboard is illustrated.

RA_1 is the reference antenna to which the ship position is determined in the MRNS. From the viewpoint of the ship antenna system, the proposed solution works in the multi-input-multi-output (MIMO) or single-input-multi-output (SIMO) mode for the vessel positioning based on multiple RBs or only one, respectively.

The receiver in the MRSN is a multi-channel device. On the one hand, this means that the signals from J RAs are fed to the receiver. On the other hand, each signal supplied from the jth RA ($j = 1, 2, ..., J$) contains the signals from K RBs that operate on K frequency sub-bands (channels). For this reason, the receiver is made in the SDR technology [37–39].

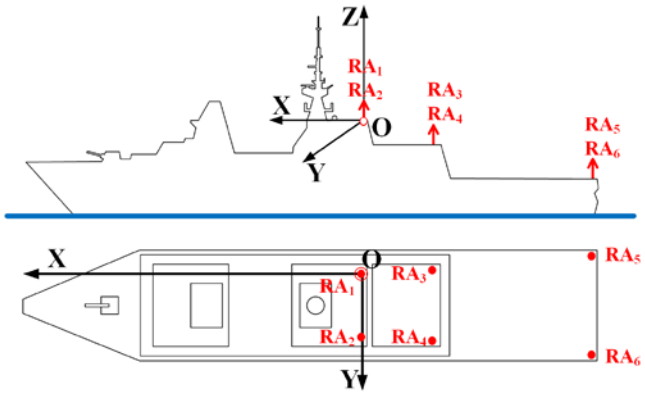

Figure 2. Exemplary arrangement of RAs on shipboard [20]

Signal processing carries out in parallel using a multi-threaded application. The signal from each antenna is divided into frequency sub-bands. For this purpose, digital filtration is carried out. In each sub-band, the information about the RB position is decoded and a Doppler frequency shift (DFS) of the received signal is determined. For each RB, estimated DFS changes versus time, so-called the Doppler curve, are the basis for determining the ship position in the SDF method.

2.4 *SDF implementation*

An analytical solution of a wave equation for a moving transmitter (Tx) in the form of relationship between the DFS and the Tx coordinates, (x_0, y_0, z_0), and time, t, [42]

$$f_{D0}(t) \cong f_{D\max} \frac{x_0 - vt}{\sqrt{(x_0 - vt)^2 + y_0^2 + z_0^2}} \tag{1}$$

is the basis of the SDF method, where $f_{D\max} = f_0 \cdot v / c$ = the maximum DFS; f_0 = the carrier frequency of the transmitted signal; v = the speed of the moving object (Tx or Rx); and c = the speed of light.

The coordinates of the emission source location may be determined based on the transformation (1) and assuming the DFS measurements in a few time-moments. In a simplified two-dimensional (2D) version of the SDF, the estimated coordinates of the localized object, $(\tilde{x}_0, \tilde{y}_0)$, are calculated on following formulas [32–34]

$$\begin{cases} \tilde{x}_0 \cong v \dfrac{t_1 A(t_1) - t_2 A(t_2)}{A(t_1) - A(t_2)} \\ \tilde{y}_0 \cong \pm \sqrt{v \left[\dfrac{(t_1 - t_2) A(t_1) A(t_2)}{A(t_1) - A(t_2)} \right]^2 - z_0} \end{cases} \tag{2}$$

where

$$A(t) = \frac{\sqrt{1 - F(t)}}{F(t)}, \quad F(t) \cong \frac{\tilde{f}_D(t)}{f_{D\max}} \tag{3}$$

where $\tilde{f}_D(t)$ and $F(t)$ = the estimated and normalized DFSs, respectively.

Equations (1)-(3) constitute the essence of the SDF. In the 2D method, it was assumed that one of the coordinates, z_0, is known. In the marine scenario, z_0 is definitely smaller (in the order of single meters) than the other two coordinates (from several hundred meters to several dozen kilometers). Thus, a difference between the transmitting and receiving antenna heights, i.e., for the analyzed RB and RA, measured against sea level is a good approximation of z_0. A three-dimensional (3D) version of the SDF is presented in [33]. In this case, a change of the object movement direction is required.

In a navigation application based on the SDF, in the first step, the coordinates of the RBs are determined in the local coordinate system associated with Rx. In the second step, the estimated coordinates of the RBs are referenced to the actual positions contained in the received signal. On this basis, the Rx (ship) position is determined.

From the technical viewpoint, two parameters, ΔT and T_A, are significant. ΔT is the analysis time of the received signal which is used to determine the instantaneous DFS. Whereas, T_A is the averaging time of the Doppler curve, which is used to estimate the localized-object coordinates, i.e., the RB. Therefore, estimation of the RB position is based on N discrete instantaneous values of the DFSs,

$$N = \left\lfloor \frac{T_A}{\Delta T} \right\rfloor \tag{4}$$

The ship coordinates are calculated in the same way as in [20]. For each k and j ($k = 1, 2, ..., K$, $j = 1, 2, ..., J$), the set of the DFSs, $f_{Dk,l}(t_n)$ ($n = 1, 2, ..., N$), creates the Doppler curve. For the positioning of each RB, the SDF uses (2) and fragments of these Doppler curves. For T_A and each jth antenna-channel (RA) of the Rx, the position of the kth RB is determined as follow [20]

$$\begin{cases} x_{\mathrm{RB}k,j} = \mathrm{v} \dfrac{t_1 A_{k,j}(t_1) - t_1 A_{k,j}(t_2)}{A_{k,j}(t_1) - A_{k,j}(t_2)} \\ y_{\mathrm{RB}k,j} = \pm \sqrt{\left[\dfrac{\mathrm{v}(t_1 - t_2) A_{k,j}(t_1) A_{k,j}(t_2)}{A_{k,j}(t_1) - A_{k,j}(t_2)} \right]^2 - z_{\mathrm{RB}k,j}^2} \\ z_{\mathrm{RB}k,j} = z_{0\mathrm{RB}k} - z_0 - z_{\mathrm{RA}j} \end{cases} \tag{5}$$

where

$$A_{k,j}(t) = \frac{\sqrt{1 - F_{k,j}^2(t)}}{F_{k,j}(t)}, \quad F_{k,j}(t) = \frac{f_{Dk,j}(t)}{f_{Dk\max}} \tag{6}$$

and $f_{Dk\max} = f_{0k} \cdot v / c$; f_{0k} = the carrier frequency of the kth RB.

Based on the kth RB signal, the vessel position is obtained by averaging and transforming (5) [20]

$$\begin{cases} x_k = \left(\frac{1}{J}\sum_{j=1}^{J}\left(x_{\mathrm{RB}k,j} + x_{\mathrm{RA}j}\right)\right)\cos\alpha \\ \quad + \left(\frac{1}{J}\sum_{j=1}^{J}\left(y_{\mathrm{RB}k,j} + y_{\mathrm{RA}j}\right)\right)\sin\alpha + x_{0\mathrm{RB}k} \\ y_k = -\left(\frac{1}{J}\sum_{j=1}^{J}\left(x_{\mathrm{RB}k,j} + x_{\mathrm{RA}j}\right)\right)\sin\alpha \\ \quad + \left(\frac{1}{J}\sum_{j=1}^{J}\left(y_{\mathrm{RB}k,j} + y_{\mathrm{RA}j}\right)\right)\cos\alpha + y_{0\mathrm{RB}k} \\ z_k = z_{0\mathrm{RB}k} - \left(\frac{1}{J}\sum_{j=1}^{J}\left(z_{\mathrm{RB}k,j} + z_{\mathrm{RA}j}\right)\right) = z_0 \end{cases} \quad (7)$$

where $\alpha = 90° - \beta$; and β = the direction of the ship movement relative to the North.

If the Rx uses only the signal from a single RB, then the current position of the ship is $(x, y, z) = (x_k, y_k, z_k)$. If the Rx receives the signals from more than one RB, the averaging process of the ship position is additionally executed. In this case, for K analyzed RBs, the weighted-mean algorithm is used [43]

$$(x, y, z) = \frac{1}{W}\left(\sum_{k=1}^{K} w_k x_k,\ \sum_{k=1}^{K} w_k y_k,\ \sum_{k=1}^{K} w_k z_k\right) \quad (8)$$

where

$$w_k = 1 - \left|\frac{1}{J}\sum_{j=1}^{J} F_{k,j}(t)\right| \quad \text{and} \quad W = \sum_{k=1}^{K} w_k \quad (9)$$

The proposed averaging algorithm considers the Doppler curve shapes and is more accurate than an arithmetic-mean [43].

3 SCENARIO AND ASSUMPTIONS FOR SIMULATION STUDIES

Simulation studies are carried out for the spatial scenario shown in Figure 3. In this case, we assumed that three RBs, marked as RB1, RB2, and RB3, are located on a shore of the Baltic Sea in localities of Łazy, Darłowo, and Jarosławiec, respectively. The position coordinates in WGS 84 and UMT for these RBs and three points, i.e., P1, P2, and P3, which determine two measurement routes, P1→P2 and P1→P3, are included in Table 1.

Table 1. Coordinates of RBs and points of beginning and ending measurement routes in WGS 84 and UMT systems (based on Google Earth Pro)

Point	WGS 84 Latitude (° N)	Longitude (° E)	UMT Northing (m N)	Easting (m E)
RB1	54.308662	16.201313	6018530	578160
RB2	54.432433	16.377603	6032510	589360
RB3	54.535533	16.540890	6044200	599700
P1	54.594149	16.553212	6050739	600353
P2	54.331924	16.028052	6020940	566850
P3	54.531990	15.867716	6043060	556150

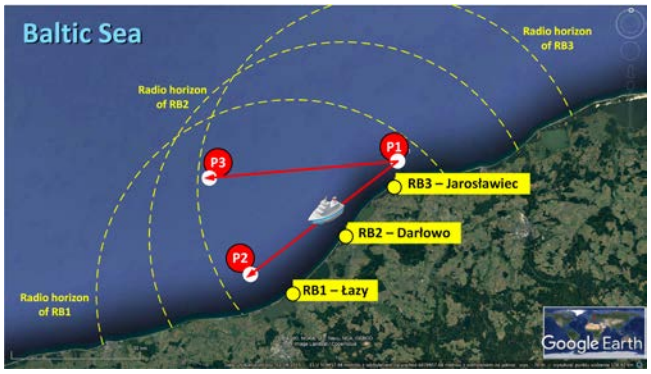

Figure 3. Spatial scenario for simulation studies (based on Google Earth Pro)

As described in Section 2.1, each RB is equipped with the telescopic mast. In simulations, the mast height is equal 50 m. For simplicity, we assumed that each vehicle with the RB is located 10 m above sea level. Hence, for all RBs, the identical antenna height is defined, i.e., $h_{Tx} = 60$ m. Location of RAs on the ship was assumed as in Figure 2, according to the assumptions shown in [20]. Assuming that the height of the lowest located RAs, i.e., for RA_5 and RA_6, is $h_{Rx} = 11$ m above sea level, then a radio horizon for each RB is about 45 km. Therefore, line-of-sight (LOS) conditions are provided in every point on two analyzed measurement routes.

Other assumptions for simulation studies are similar to shown in [20]. The RBs transmit PSK signals with bandwidth $B = 200$ kHz at frequencies $f_{01} = 1860$ MHz, $f_{02} = 1860.3$ MHz, and $f_{03} = 1860.6$ MHz, respectively for RB1, RB2, and RB3. On the frequencies $f_{0k} + 0.75B$, $k = 1, 2, 3$, the pilot signal used in the SDF is additionally transmitted. The minimum carrier-to-noise ratio is $CNR_{\min} = 5$ dB. The basic frequency of the spectral analysis is 1 mHz. Additionally, we adopted $\Delta T = 1$ s and $T_A = 240$ s. The speed of the ship relative to land is $v = 20$ w. ≅ 10.3 m/s.

4 RESULTS OF SIMULATION STUDIES

The purpose of the carried out simulation tests is to assess the positioning accuracy and to present several aspects of the SDF use in the MRNS. In Section 4.1, the comparison of the arithmetic and weighted averaging the ship coordinates is shown. This analysis is based on the results obtained for the measurement route P1→P2. Section 4.2 contains a comparison of the

positioning results at two considered measurement routes.

The basic measure of positioning accuracy is the position error defined as follows [33]

$$\Delta R = \sqrt{(x - x_0)^2 + (y - y_0)^2 + (z - z_0)^2} \tag{10}$$

where (x, y, z) and (x, y, z) = the estimated and real coordinates of the vessel, respectively.

4.1 *Comparison of arithmetic and weighted averaging*

The simulation studies are carried out for the measuring route P1→P2 and the assumptions described in Section 3. Figures 4 and 5 show the ship position at the route based on the arithmetic and weighted averaging, respectively. Additionally, average position errors for the entire route are marked with dashed lines.

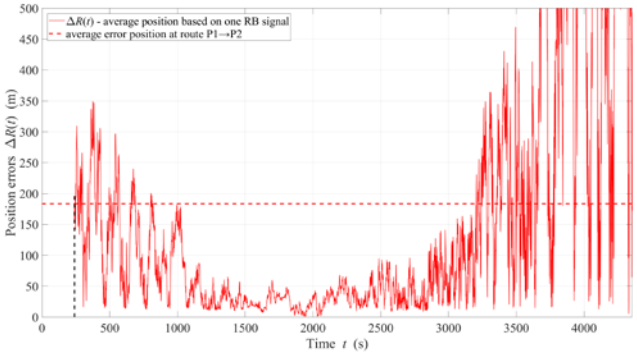

Figure 4. Ship position error at route P1→P2 using arithmetic averaging

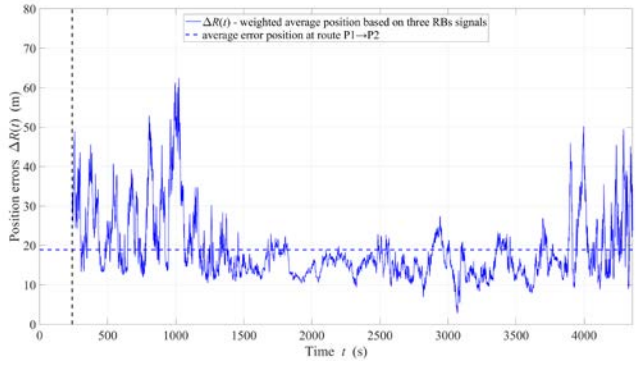

Figure 5. Ship position error at route P1→P2 using weighted averaging

The obtained results of the measure ΔR show that the application of the weighted average described by (8) is more effective than the arithmetic average. In the case of the weighted averaging, the ship position error on the route P1→P2 does not exceed 70 m. The average error on the entire route can be used to compare both methods. These errors are equal to 18.9 m and 183.6 m for the weighted and arithmetic averages, respectively.

In order to assess the qualitative positioning of the ship using the two analyzed averaging methods, a cumulative distribution function (CDF) is determined for the position error, $F(\Delta R)$. These CDFs are illustrated in Figure 6. The results obtained confirm the greater accuracy of estimating the ship position using the weighted average.

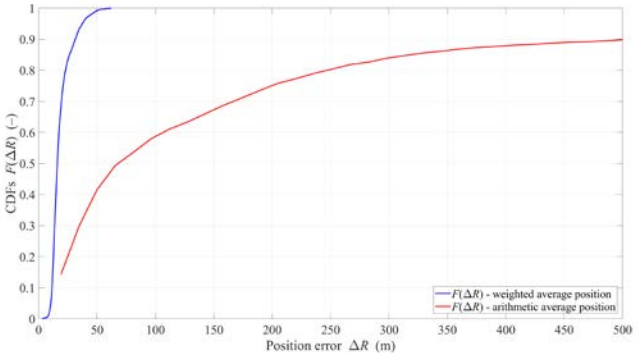

Figure 6. CDFs of ship position error at route P1→P2 for two averaging methods

4.2 *Comparison of ship positioning at different measurement routes*

The two measurement routes shown in Figure 3 differ in their location relative to three analyzed RBs. This transfers into other Doppler curves for three RBs obtained in the ship receiver at the individual measurement routes. Changes of the theoretical DFSs calculated based on (1) are depicted in Figures 7 and 8 for the routes P1→P2 and P1→P3, respectively.

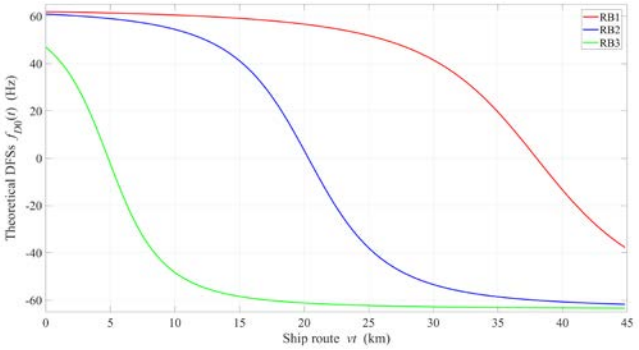

Figure 7. Doppler curves for route P1→P2

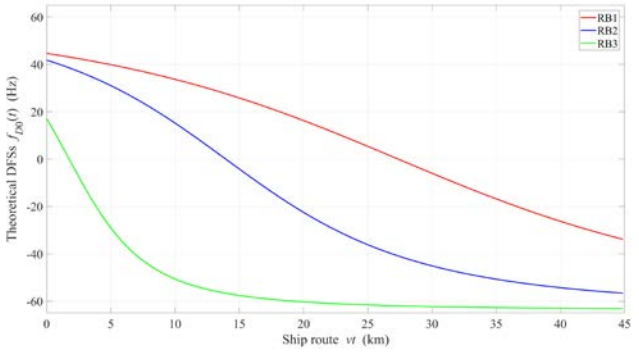

Figure 8. Doppler curves for route P1→P3

Based on the shown Doppler curves, we can see that the DFSs changes are more diverse for the route

P1→P2. Using the weighted average in the SDF reduces the impact of the DFS variability on the positioning accuracy.

In Figure 9, the vessel position error along its movement trajectory at the route P1→P3 for the weighted average is illustrated. Analogous results for the route P1→P2 are depicted in Figure 5.

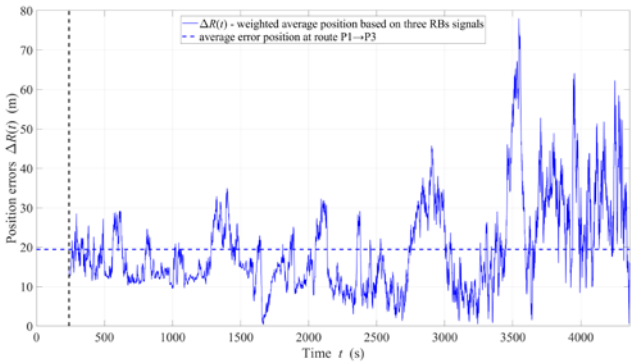

Figure 9. Ship position error at route P1→P3 using weighted averaging

Due to the weighted average, the results obtained for both routes are similar. In this case, the average error for the entire route is equal to 19.5 m. This is also clearly visible in the CDF graphs shown in Figure 10.

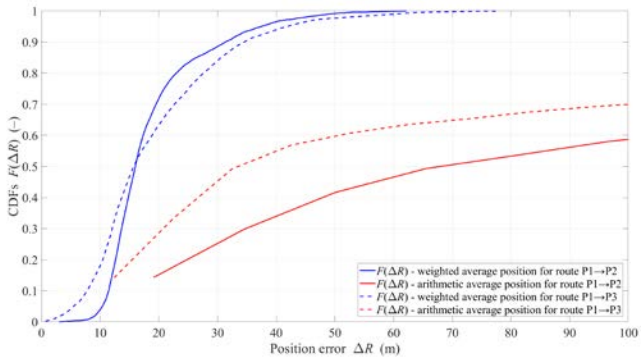

Figure 10. CDFs for two analyzed routes

The obtained results confirm the effectiveness of using the SDF method for the vessel positioning in the coastal zone.

5 CONCLUSION

In this paper, the concept of using the mobile RBs in the backup navigation system for the vessels in the coastal zone was presented. Such the system may be especially used in the denied-GNSS conditions. In the paper, we have outlined the major differences between the SDF-based stationery and mobile navigation systems. The effectiveness of the MRNS was confirmed based on the simulation studies for two selected measurement routes and three mobile RBs. The use of the weighted average in the SDF method allows for decreasing the ship positioning errors. In this case, the average position error was less than 20 m for the analyzed measurement scenario. The obtained results coincide with those presented for the stationary backup system [20].

ACKNOWLEDGMENTS

This work was developed within a framework of the Research Grant "Basic research in sensor technology field using innovative data processing methods" no. GBMON/13-996/2018/WAT sponsored by the Polish Ministry of Defense.

REFERENCES

[1] Groves, P.D. 2013. Principles of GNSS, inertial, and multisensor integrated navigation systems, 2nd ed. Boston, MA, USA: Artech House.
[2] Dardari, D., Luise, M., & Falletti E. (eds) 2016. Satellite and terrestrial radio positioning techniques: A signal processing perspective. Oxford, UK: Academic Press, 2016.
[3] Blanchard, W. 2015 The genesis of the Decca Navigator System. The Journal of Navigation 68(2): 219–237.
[4] Swanson, E.R. 1983. Omega. Proceedings of the IEEE 71(10): 1140–1155.
[5] Specht, C., Weintrit, A. & Specht, M. 2016. A history of maritime radio-navigation positioning systems used in Poland. The Journal of Navigation 69(3): 468–480.
[6] Proc, J. 2018. Hyperbolic radionavigation systems. Available: http://jproc.ca/hyperbolic/.
[7] Kayton, M. & Fried, W.R. 1997. Avionics navigation systems, 2nd ed. New York, NY, USA: Wiley-Interscience.
[8] van Diggelen, F. 2009. A-GPS: Assisted GPS, GNSS, and SBAS. Boston, MA, USA: Artech House, 2009.
[9] Kaplan, E.D. 2005. Understanding GPS: Principles and applications, 2nd ed. Boston, MA, USA: Artech House.
[10] Chan Y.T. & Ho, K.C. 1994. A simple and efficient estimator for hyperbolic location. IEEE Transactions on Signal Processing 42(8): 1905–1915.
[11] López, M. & Antón, V. 2018. SBAS/EGNOS enabled devices in maritime. TransNav, the International Journal on Marine Navigation and Safety of Sea Transportation 12(1): 23–27.
[12] IERS. 2019. Doppler Orbitography and Radiopositioning Integrated by Satellite (DORIS). Available: https://www.iers.org/IERS/EN/Science/Techniques/doris.html.
[13] Basker, S., Williams, P., Bransby, M., Last, J.D., Offermans, G. & Helwig, A. 2008. Enhanced Loran: Real-time maritime trials. 2008 IEEE/ION Position, Location and Navigation Symposium (PLANS), Monterey, CA, USA, 11–14 April 2008: 792–799.
[14] Offermans, G., Johannessen, E., Bartlett, S., Schue, C., Grebnev, A., Bransby, M., Williams, P., Hargreaves, C. 2015. eLoran initial operational capa-bility in the United Kingdom – First results. 2015 International Technical Meeting of the Institute of Navigation, Dana Point, CA, USA, 26–29 January 2015: 27–39.
[15] Küpper, A. 2005. Location-based services: Fundamentals and operation. Chichester, England; Hoboken, NJ, USA: Wiley.
[16] Iyidir, B. & Ozkazanc, Y. 2004. Jamming of GPS receivers. IEEE 2004 12th Signal Processing and Communications Applications Conference (SIU), Kusadasi, Turkey, 30–30 April 2004: 747–750.
[17] Magiera, J. & Katulski, R.J. 2013. Accuracy of differential phase delay estimation for GPS spoofing detection. 2013 36th International Conference on Telecommunications and Signal Processing (TSP), Rome, Italy, 2–4 July 2013: 695–699.

[18] Magiera, J. & Katulski, R.J. 2014. Applicability of null-steering for spoofing mitigation in civilian GPS. 2014 IEEE 79th Vehicular Technology Conference (VTC Spring) Seoul, South Korea, 18–21 May 2014: 1–5.
[19] Magiera, J. & Katulski, R.J. 2015. Detection and mitigation of GPS spoofing based on antenna array processing. Journal of Applied Research and Technology 13(1): 45–57.
[20] Kelner, J.M., Ziółkowski, C., Nowosielski, L. & Wnuk, M. 2016. Reserve navigation system for ships based on coastal radio beacons. 2016 IEEE/ION Position, Location and Navigation Symposium (PLANS), Savannah, GA, USA, 11–14 April 2016: 393–402.
[21] OBR CTM S.A. 2019. Research and Development Center for Maritime Technology (in Polish: Ośrodek Badawczo-Rozwojowy Centrum Techniki Morskiej S.A.). Available: https://ctm.gdynia.pl/en/.
[22] Ambroziak, S.J., Katulski, R.J., Sadowski, J., Siwicki, W. & Stefański, J. 2011. Asynchronous and self-organizing radiolocation system – AEGIR. 2011 IEEE International Conference on Technologies for Homeland Security (HST), Waltham, MA, USA, 15–17 November 2011: 419–425.
[23] Ambroziak, S.J., Katulski, R.J., Sadowski, J., Siwicki, W. & Stefański, J. 2012. Ground-based radiolocation system – AEGIR. 2012 8th International Symposium on Mechatronics and its Applications (ISMA), Sharjah, United Arab Emirates, 10–12 April 2012: 1–5.
[24] Ambroziak S.J., Katulski R.J., Sadowski J., Siwicki W., Stefański J.: Ground-based, Hyperbolic Radiolocation System with Spread Spectrum Signal - AEGIR. TransNav, the International Journal on Marine Navigation and Safety of Sea Transportation, Vol. 5, No. 2, pp. 233-238, 2011.
[25] Duckworth G.L. & Baranoski, E.J. 2007. Navigation in GNSS-denied environments: Signals of opportunity and beacons. Military Capabilities Enabled by Advances in Navigation Sensors. Meeting Proceedings RTO-MP-SET-104, Neuilly-sur-Seine, France, 2007: 3-1–3-14.
[26] Panigrahi, N., Doddamani, S.R., Singh, M. & Kandulna, B.N. 2015. A method to compute location in GNSS denied area. 2015 IEEE International Conference on Electronics, Computing and Communication Technologies (CONECCT), Bangalore, India, 10–11 July 2015: 1–5.
[27] Zahran, S., Moussa, A. & El-Sheimy, N. 2018. Enhanced UAV navigation in GNSS denied environment using repeated dynamics pattern recognition. 2018 IEEE/ION Position, Location and Navigation Symposium (PLANS), Monterey, CA, USA, 23–26 April 2018: 1135–1142.
[28] Chevli, K.R., Kim, P.Y., Kagel, A.A., Moy, D.W., Pattay, R.S., Nichols, R.A. & Goldfinger, A.D. 2006. Blue force tracking network modeling and simulation. 2006 IEEE Military Communications Conference (MILCOM), Washington, DC, USA, 23–25 October 2006: 1–7.
[29] Shridharan, S., Kumar, R. & Pundir, S.K. 2013. Positioning of military combat units through weight-based terrain analysis using NASA World Wind. 2013 IEEE Symposium on Computational Intelligence for Security and Defense Applications (CISDA), Singapore, 16–19 April 2013: 9–15.
[30] Kelner, J.M. & Ziółkowski, C. 2012. Autonomous system of monitoring location and identification of individual soldiers in subunits of own forces (in Polish). 2012 IX Conference on Reconnaissance and Electronic Warfare Systems (CREWS), Kazimierz Dolny, Poland, 6–8 November 2012: 1–11.
[31] Jacobus, C.J., Cohen, C., Haanpaa, D. & Siebert, G. A personal blue force tracking system.
[32] Kelner, J.M., Ziółkowski, C. & Kachel, L. 2008. The empirical verification of the location method based on the doppler effect. 2008 17th International Conference on Microwaves, Radar and Wireless Communications (MIKON), Wrocław, Poland, 19–21 May 2008. vol. 3: 755–758.
[33] Kelner, J.M. 2010. Analysis of the Doppler location method of the radio waves emission sources, Ph.D. Thesis (in Polish). Warsaw, Poland: Military University of Technology.
[34] Gajewski, P., Ziółkowski, C. & Kelner, J.M. 2012. Using SDF method for simultaneous location of multiple radio transmitters. 2012 19th International Conference on Microwave Radar and Wireless Communications (MIKON), Warsaw, Poland, 21–23 May 2012. vol. 2: 634–637.
[35] COSPAS-SARSAT. 2019. International COSPAS-SARSAT Programme. Available: https://cospas-sarsat.int/en/.
[36] Levanon, N. & Ben-Zaken, M. 1985. Random error in ARGOS and SARSAT satellite positioning systems. IEEE Transactions on Aerospace and Electronic Systems AES-21(6): 783–790.
[37] Arslan, H. 2007. Cognitive radio, software defined radio, and adaptive wireless systems. Dordrecht, Netherlands: Springer.
[38] Wyglinski, A.M. & Pu, D. 2013. Digital communication systems engineering with software-defined radio. Boston, MA, USA; London, UK: Artech House.
[39] Kelner, J.M., Ziółkowski, C. & Marszałek, P. 2016. Influence of the frequency stability on the emitter position in SDF method. 2016 17th International Conference on Military Communications and Information Systems (ICMCIS), Brussels, Belgium, 23-24 May 2016: 1–6.
[40] Kelner, J.M. & Ziółkowski, C. 2015. The use of SDF technology to BPSK and QPSK emission sources' location. Przegląd Elektrotechniczny 91(3): 61–65.
[41] Rafa, J. & Ziółkowski, C. 2008. Influence of transmitter motion on received signal parameters – Analysis of the Doppler effect. Wave Motion 45(3): 178–190.
[42] Kelner, J.M. 2011. Positioning an aircraft using the TDSDF method. Polish Journal of Environmental Studies 20(5A): 80–84.